

Journal of  
**Micro/Nanolithography,  
MEMS, and MOEMS**

Nanolithography.SPIEDigitalLibrary.org

**Optical fiber strain sensor based on  
sandwiched long-period fiber  
gratings with a surface bonding layer**

Chia-Chin Chiang  
Chien-Hsing Li

# Optical fiber strain sensor based on sandwiched long-period fiber gratings with a surface bonding layer

Chia-Chin Chiang\* and Chien-Hsing Li

National Kaohsiung University of Applied Sciences, Department of Mechanical Engineering, 415 Chien Kung Road, Kaohsiung 807, Taiwan

**Abstract.** An optical fiber strain sensor based on sandwiched long-period fiber gratings (OFSS-SLPFG) with a surface bonding layer is proposed. The proposed OFSS-SLPFG is an etched optical fiber that is sandwiched between two thick photoresists with a periodic structure. To prevent the glue effect in the surface bonding process, where glue flows into the SLPFG structure, reducing the coupling strength, a surface bonding layer (thickness: 16  $\mu\text{m}$ ) is used as the base layer on the bottom of the OFSS-SLPFG. The OFSS-SLPFG is, therefore, more effective for use as a strain sensor. When external strain loading is applied, the resonant dip loss of the OFSS-SLPFG is reflected linearly. A bending strain calibration experiment is demonstrated by the four-point bending test. The results show an average linearity ( $R^2$ ) of 0.980, with a sensitivity of 0.00788 dB/ $\mu\text{E}$ . This phenomenon suggests that the OFSS-SLPFG can be utilized as a sensitive strain transducer. © The Authors. Published by SPIE under a Creative Commons Attribution 3.0 Unported License. Distribution or reproduction of this work in whole or in part requires full attribution of the original publication, including its DOI. [DOI: 10.1117/1.JMM.13.4.043008]

Keywords: optical fiber sensor; strain; long-period fiber gratings.

Paper 14041 received Apr. 9, 2014; revised manuscript received Sep. 25, 2014; accepted for publication Oct. 3, 2014; published online Nov. 3, 2014.

## 1 Introduction

Strain sensing is especially important as an engineering application. Normally, the resistance strain gauge is used in strain sensing. The coil resistance strain gauge utilizes the change of resistance with deformation via the bridge balance. Poor electromagnetic and corrosion resistances, however, are the disadvantages of the coil strain gauge. With its high sensitivity, small size, and electromagnetic resistance, the long-period fiber grating (LPFG) sensor is more applicable for sensing strain,<sup>1–4</sup> temperature,<sup>5,6</sup> pressure,<sup>7</sup> and dispersion compensation.<sup>8</sup>

Fabrication methods for LPFG include the amplitude mask method,<sup>9</sup> CO<sub>2</sub> laser method,<sup>10</sup> arc method,<sup>11</sup> mechanical pressure method,<sup>12</sup> and etching method.<sup>13</sup> The most common fabrication method for LPFG is fabrication via UV excimer laser photoimprint<sup>9</sup> to form refractive index modulations. The disadvantages of this UV method include the use of expensive apparatuses and that it is unsuitable for mass production. In 2010, the sandwiched long-period fiber grating (SLPFG) was first reported<sup>14</sup> as a loss tunable filter made via the thick photoresist process. The SLPFG structure consists of an etched optical fiber that is sandwiched between two thick photoresists with a periodic structure. This process of the SLPFG not only improves the overall performance of traditional fiber grating, but also cuts down on fabrication costs.

In a 1992 study on an LPFG-based optical sensor, Vaziri and Chen<sup>1</sup> proposed an etch method to fabricate fiber gratings as a strain gauge. However, the strength of this type of sensor is questionable because the fiber is etched without packaging. In 2006, Wang et al.<sup>3</sup> presented a LPFG strain sensor with a low temperature sensitivity. In that research, LPFGs were fabricated with a CO<sub>2</sub> laser, and the strain sensitivity and temperature were  $-7.6 \text{ pm}/\mu\text{E}$  and  $3.91 \text{ pm}/^\circ\text{C}$ ,

respectively. Nevertheless, this method is not suitable for surface bonding because glue decreases the LPFG coupling strength so that the resonant dip vanishes at certain refractive indices. When the sensor is surface bonded with glue, problems in strain sensing applications are created.

The current work shows that this glue problem can be avoided by using a 16- $\mu\text{m}$  surface bonding layer on the SLPFG. A strain calibration is made on the optical fiber strain sensor based on a sandwiched long-period fiber grating (OFSS-SLPFG) sensor to obtain strain sensitivity.

## 2 Theory

The resonant dip loss of the SLPFG can be tuned by the loadings for loss tunable filter applications.<sup>14</sup> When external loading is applied on the SLPFG, the strain will be raised according to the section of the structure on which the loading is applied. The resulting periodic refractive index variance in the fiber core forms a spectrum with LPFG characteristics. Loading can tune the resonant dip loss (attenuation) of the SLPFG. By monitoring the SLPFG resonant dip loss, the proposed device has potential for high-speed, intensity-based, strain-sensing system, and communication applications.

In this study, grating periods of 670  $\mu\text{m}$  were designed for SLPFG resonance-attenuation wavelengths at 1550 nm. Figure 1 shows the dimensional parameters of the OFSS-SLPFG, indicating a 30-mm gauge length, 670- $\mu\text{m}$  period, 73- $\mu\text{m}$  diameter for the etched region, and an unetched diameter of 125  $\mu\text{m}$ .

The present study used a four-point bending device for strain calibration. When the beam is bent with the four-point bending device, the central section is under a purely axial tensile strain at the surface. As the external tensile strain is applied, the strain increases accordingly in different sections of the SLPFG. Thus, a periodic refractive index variance in the fiber core is obtained. As a result, the spectra of the SLPFG deform because of the strain, and the attenuation loss of the SLPFG can be changed with the strain in the sensing applications.

\*Address all correspondence to: Chia-Chin Chiang, E-mail: cchiang@cc.kuas.edu.tw

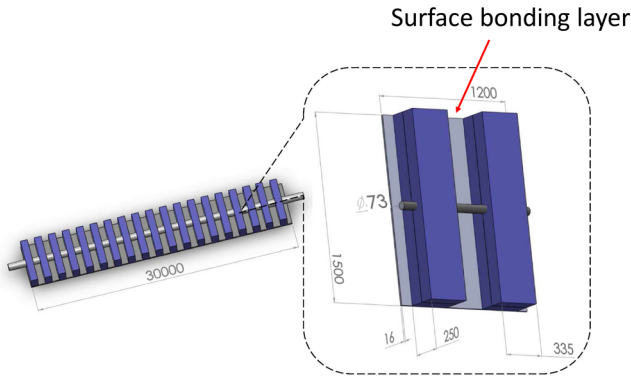


**Fig. 1** Schematic diagram indicating the sizes of the different parts of the optical fiber strain sensor based on sandwiched long-period fiber gratings (OFSS-SLPFG).

When the beam is bent by the four-point device, the central section then bends without shear stress. The axial tensile stress is as follows:

$$\sigma = E\varepsilon = \frac{My}{I}, \tag{1}$$

where  $\sigma$  is the bending stress,  $I$  is the moment of inertia,  $\varepsilon$  is the strain,  $M$  is the moment, and  $y$  is the distance from the neutral axis to the point where the bending strain is applied.

The schematic diagrams of the four-point bending and the bending moment diagram are shown in Fig. 2. The bending moment of the central section of four-point bending ( $M$ ) is constant and equal to  $PL_{1/2}$ . By substituting that value into Eq. (1), we can obtain the bending stress.

By adopting the moment-area method, we can calculate the bending stress using the maximum deflection. The

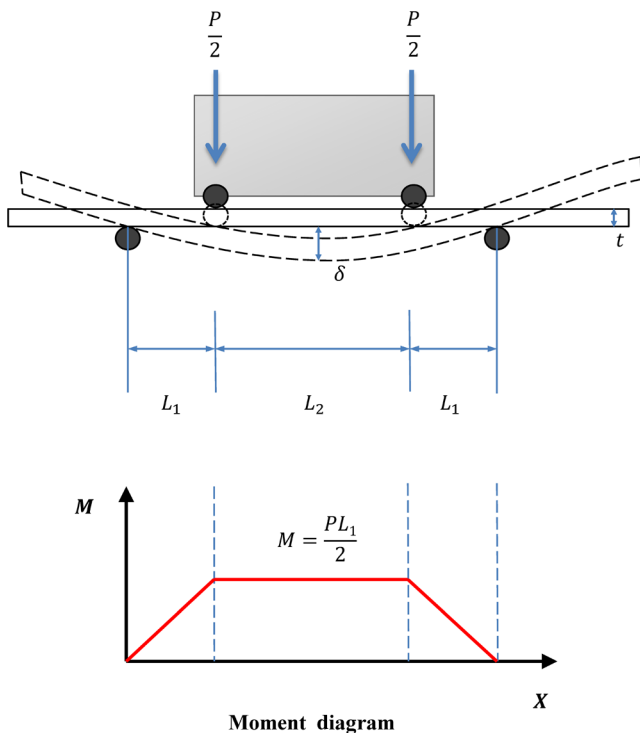


**Fig. 2** Schematic diagram of the four-point bending moment.

bending stress is referred to in the G39-99 specification of the American Society for Testing and Materials.<sup>15</sup> The bending stress equation is

$$\sigma = \frac{12Et\delta_{\max}}{3H^2 - 4A^2}, \tag{2}$$

where  $H$  is the distance for the external two support points,  $A$  is the side on which the two internal forces are applied, and  $\delta_{\max}$  is the maximum deformation.

The present study uses a four-point bending force module and end-support mining equidistant cylindrical design, where  $A = L_2$ , and  $H = 2L_1 + L_2$ ; the substituted bending stress equation can be rewritten as

$$\varepsilon = \frac{12t\delta_{\max}}{3L_1^2 + 3L_1L_2 - L_2^2}. \tag{3}$$

According to the couple mode theory<sup>14</sup> for SLPFG, the transmission loss in Eq. (4) is

$$T = \cos^2(\kappa_{\text{co-cl}}^{\text{ac}}L), \tag{4}$$

where  $T$  is the transmission loss of an SLPFG,  $L$  indicates the length of the SLPFG, and  $\kappa_{\text{co-cl}}^{\text{ac}}$  is the AC component of the coupling coefficient between the core and the cladding. The transmission loss of an SLPFG can be deduced from the AC component of the coupling coefficient between the core and the cladding. The transmission loss of an SLPFG is a cosine-squared equation. Transmission loss is a function of  $\kappa_{\text{co-cl}}^{\text{ac}}$ , which is proportional to the amplitude of changes in the refractive index because of variation in the strain field. Therefore, the loss can be changed by external loading. From Eq. (4), we can measure the strain by monitoring the transmission loss of the OFSS-SLPFG.

### 3 Processing of OFSS-SLPFG

The lithography and etching processes for fabricating OFSS-SLPFG are shown in Fig. 3. First, copper is deposited by sputtering on the surface of the wafer [4 in. (100)] as a sacrificial layer for the wet-etching release of SLPFG. Second, the SU-8 10 photoresist is spin coated on the wafer to create a 16- $\mu\text{m}$ -thick OFSS-SLPFG base layer used as the surface bonding layer to prevent the glue effect. Third, the 120- $\mu\text{m}$ -thick negative photoresist SU-8 3050 is spun on the base layer, and the supporting structure is developed via lithography as the second layer for the bottom grating pattern. After forming the supporting structures, the etched optical fiber with a 73- $\mu\text{m}$  diameter is precisely fixed to the supporting structure. Then, the 130- $\mu\text{m}$  photoresist SU-8 3050 is spun again to cover the optical fiber and form the third layer. The fiber, which is embedded in a patterned SU8 3050 photoresist, is attained by means of this process. Fourth, the sacrificial copper thin film is removed with a solution of 45% ferric chloride, completing the OFSS-SLPFG.

### 4 Experimental Setup

In this study, an OFSS-SLPFG and a coil strain gauge were surface bonded to an aluminum sheet specimen ( $150 \times 25 \times 2 \text{ mm}^3$ ), with the screw manually rotated to apply the bending strain in the four-point bending test. The experimental setup consisted of a broadband light source (wavelength 1400 to 1650 nm), an optical spectrum analyzer

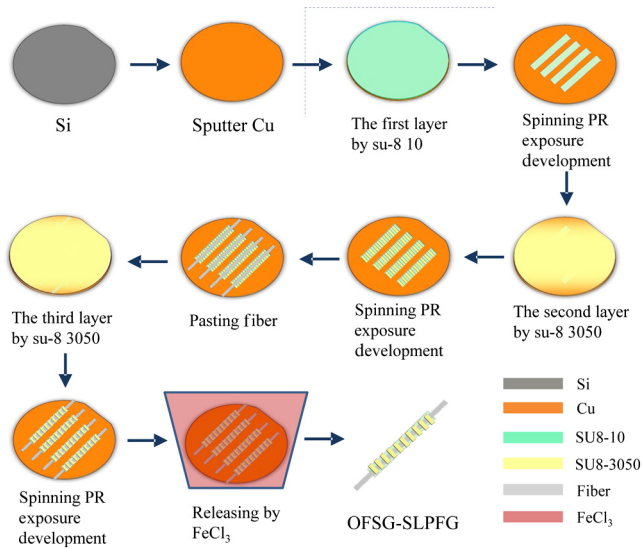


Fig. 3 The OFSS-SLPFG fabrication process.

(MS9710C), the OFSS-SLPFG, the coil strain gauge (gauge factor: 2.08; gauge resistance:  $120.4 \pm 0.4\Omega$ ), the four-point bending module, a Wheatstone bridge, signal acquisition systems, and personal computers. Using an optical signal generated by the broadband light source and passing through the OFSS-SLPFG, the optical spectrum analyzer could function as a receiver and monitor the spectra of the OFSS-SLPFG in the bending test. The strain gauge signal was read by the Wheatstone bridge and connected to the signal acquisition system using LabView software to retrieve the strain values. A schematic diagram of the experimental setup is shown in Fig. 4.

### 5 Results and Discussion

The proposed OFSS-SLPFG is a sandwiched long period fiber grating strain sensor with a surface bonding layer which serves as the base layer on the bottom of the OFSS-SLPFG to prevent the glue effect in the surface bonding process. Figure 5 shows the glue flow in the structure of an SLPFG without a surface bonding layer after the surface bonding process. The glue causes the LPFG coupling strength to decrease so that the resonant dip vanishes after the surface bonding process. An scanning electron microscopy graph of the OFSS-SLPFG with a surface bonding layer is shown in Fig. 6. The surface bonding layer of the

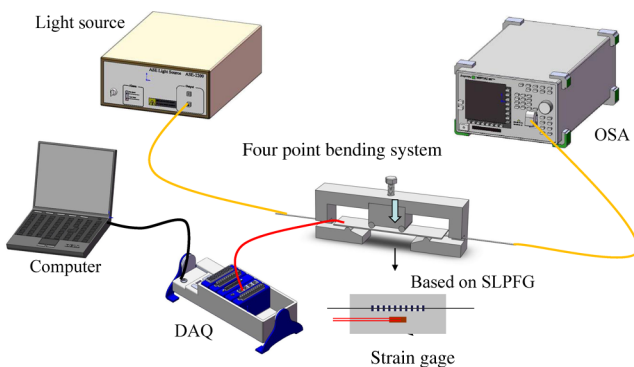


Fig. 4 Experimental setup of the four-point bending test.

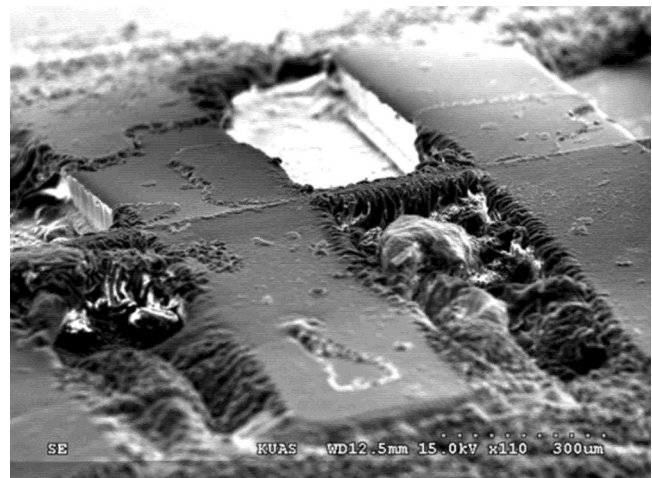


Fig. 5 The glue flow in the structure of an SLPFG without a surface bonding layer after the surface bonding process.

OFSS-SLPFG prevents the glue from flowing into the structure of the OFSS-SLPFG strain sensor. The OFSS-SLPFG is, therefore, more effective for use as a strain sensor.

Based on the four-point bending test, we applied the strain on the sensors by rotating the screw. The relationship of the screw displacement and applied strain on the central section surface of the specimen was linear, as shown in Fig. 7. The slope of the linear curve was  $544.7 \mu\epsilon/\text{mm}$ , and the  $R^2$  value was 0.996. This phenomenon means that the screw displacement and the applied strain show a significant linear and stable relationship.

Figure 8 illustrates the transmission spectra of the OFSS-SLPFG with various applied strains. The development of transmission dips can be observed from the spectra of the OFSS-SLPFG with various strains. After surface bonding, glue will be induced for the residual strain on OFSS-SLPFG. Therefore, the transmission spectrum of the surface bonding OFSS-SLPFG has a resonant dip of  $-10.26 \text{ dB}$  at  $1555.750 \text{ nm}$ . When the strain loading of the OFSS-SLPFG increases, the transmission dip will deform and grow with various strains. The dips of the OFSS-SLPFG grow linearly

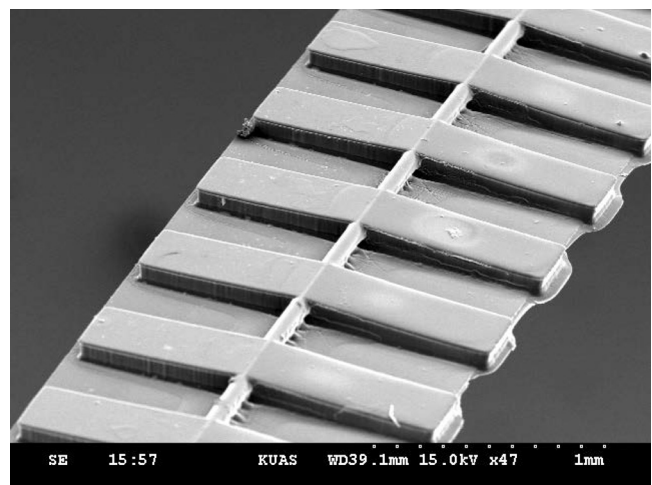


Fig. 6 The surface bonding layer of the OFSS-SLPFG prevents the glue from flowing into the structure of the sensor.

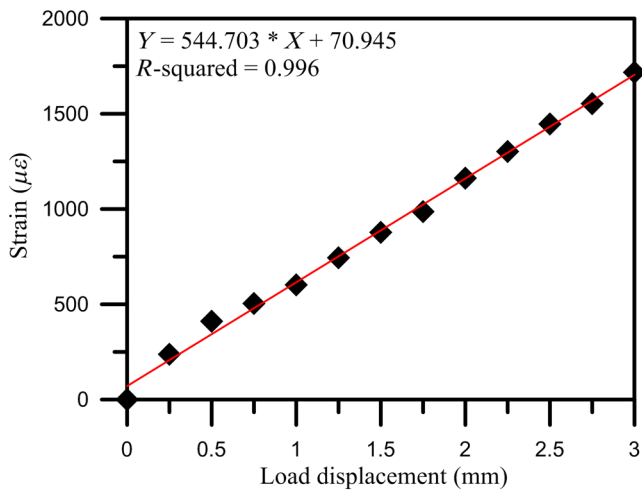


Fig. 7 The relationship of screw displacement and strain.

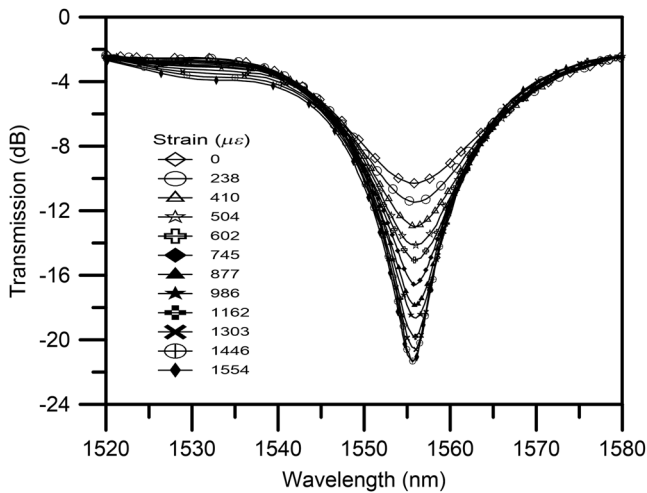


Fig. 8 The transmission spectra of the OFSS-SLPFG with various applied strains.

up to the maximum transmission loss. The maximum transmission dip of the OFSS-SLPFG is  $-21.42$  dB at  $1555$  nm under an applied strain of  $1554$   $\mu\epsilon$  loading. The linear relation of transmission dips to applied strain is shown in Fig. 9. The sensitivity reaches  $-0.00788$  dB/ $\mu\epsilon$  and the linearity  $R^2$  is about 0.980. The proposed OFSS-SLPFG can be used as a strain sensor by monitoring the attenuation loss. Therefore, the proposed OFSS-SLPFG has the potential for high speed strain sensing by intensity modulation.

During the four-point bending test, the position of the resonant wavelength shift was not as obvious as is shown in Fig. 9. The center wavelength was  $1555.750$  nm under the condition of surface bonding with free strain loading. When the OFSS-SLPFG was under a loading of  $1554$   $\mu\epsilon$ , the wavelength was shifted about  $0.750$  nm. As demonstrated in Fig. 9, the curve of the wavelength and applied strain was linear, with a small slope of about  $0.000234$  nm/ $\mu\epsilon$ . The linearity  $R^2$  was about 0.471, which was lower than the resonant dip-strain relation. Consequently, the resonant dip-strain relation is more suitable for strain sensing applications.

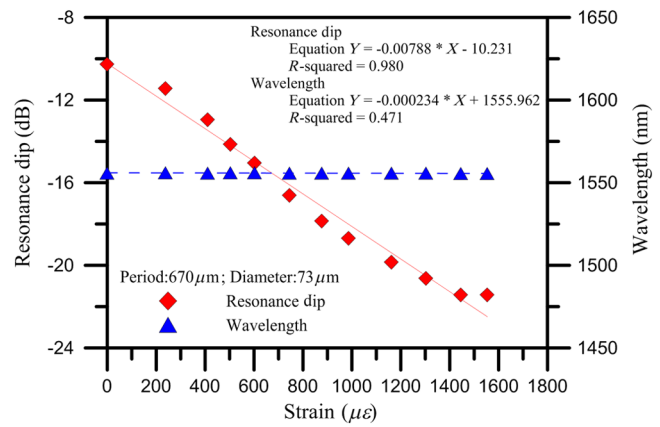


Fig. 9 Transmission and resonance wavelength versus applied strain.

## 6 Conclusions

The OFSS-SLPFG is demonstrated. The four-point bending test was adopted to conduct the strain calibration with a strain sensitivity of  $-0.00788$  dB/ $\mu\epsilon$  and  $R^2$  of 0.980. Moreover, the results show that the proposed OFSS-SLPFG has potential for high sensitivity strain sensing.

## Acknowledgments

The work is supported by the Ministry of Science and Technology, Taiwan (grant number MOST-103-2221-E-151-009-MY3).

## References

1. M. Vaziri and C. L. Chen, "Etched fibers as strain gauges," *J. Lightwave Technol.* **10**(6), 836–841 (1992).
2. B. Vikram et al., "Temperature-insensitive and strain-insensitive long-period grating sensors for smart structures," *Opt. Eng.* **36**(7), 1872–1876 (1997).
3. Y. P. Wang et al., "Highly sensitive long-period fiber-grating strain sensor with low temperature sensitivity," *Opt. Lett.* **31**(23), 3414–3416 (2006).
4. A. Sun and Z. Wu, "Hybrid long-period-grating and fiber Bragg grating for cladding-mode-recoupling-based discrimination of temperature and strain," *Opt. Eng.* **51**(4), 044402 (2012).
5. Y. G. Han and S. B. Lee, "Compositional dependence of the temperature sensitivity in long-period fiber gratings with doping concentration of GeO<sub>2</sub> and B<sub>2</sub>O<sub>3</sub> and their applications," *Opt. Eng.* **43**(5), 1144–1147 (2004).
6. J. Huang et al., "Reflection-based phase-shifted long period fiber grating for simultaneous measurement of temperature and refractive index," *Opt. Eng.* **52**(1), 014404 (2013).
7. Y. F. Zhang et al., "Tilted long period gratings pressure sensing in solid core photonic crystal fibers," *IEEE Sens. J.* **12**(5), 954–957 (2012).
8. M. Das and K. Thyagarajan, "Dispersion compensation in transmission using uniform long period fiber gratings," *Opt. Commun.* **190**(1–6), 159–163 (2001).
9. V. Bhatia and A. M. Vengsarkar, "Optical fiber long-period grating sensors," *Opt. Lett.* **21**(9), 692–694 (1996).
10. D. D. Davis et al., "Long-period fibre grating fabrication with focused CO<sub>2</sub> laser pulses," *Electron. Lett.* **34**(3), 302–303 (1998).
11. I. K. Hwang, S. H. Yun, and B. Y. Kim, "Long-period fiber gratings based on periodic microbends," *Opt. Lett.* **24**(18), 1263–1265 (1999).
12. S. Savin et al., "Tunable mechanically induced long-period fiber gratings," *Opt. Lett.* **25**(10), 710–712 (2000).
13. C. C. Chiang, H. J. Chang, and J. S. Kuo, "Novel fabrication method of corrugated long-period fiber gratings by thick SU-8 photoresist wet-etching technique," *J. Micro/Nanolith. MEMS MOEMS* **9**(3), 033007 (2010).
14. C. C. Chiang et al., "Sandwiched long-period fiber grating filter based on periodic SU8-thick photoresist technique," *Opt. Lett.* **34**(23), 3677–3679 (2009).
15. ASTM Standard G39, *Standard Practice for Preparation and Use of Bent-Beam Stress-Corrosion Test Specimens*, ASTM International, West Conshohocken, Pennsylvania (2005).

**Chia-Chin Chiang** received his PhD degree from National Taiwan University in 2005. Since 2011, he has been an associate professor with the Department of Mechanical Engineering of National Kaohsiung University of Applied Sciences. His research interests include fiber Bragg gratings, optical fiber sensors, and smart materials and structures.

**Chien-Hsing Li** received an MS degree in the Department of Mechanical Engineering from National Kaohsiung University of Applied Sciences in 2014. His research interests include fiber-optic sensors and micro-electromechanical systems.